Numerical Simulation of Detritiation System for NIFS with Commercial Catalyst and Adsorbent

K. Munakata[a,*], K. Hara[a], T. Sugiyama[b], K. Kotoh[c], M. Tanaka[d] and T. Uda[d]
*kenzo @gipc.akita-u.ac.jp
[a] Faculty of Engineering and Resource Science, Akita University, Tegata-gakuen-machi 1-1, AKITA 010-8502 Japan
[b] Nagoya University, Furo-cho Chikusa-ku, Nagoya464-8603, Japan
[c]Kyushu University, Motooka 744, Nishi-ku, Fukuoka 819-0395, Japan
[d]National Institute for Fusion Science, Oroshi-cho 322-6, Toki, Gifu 509-5292 Japan

(Received: 9 May 2012 / Accepted: 18 August 2012)

Establishment of tritium recovery system is necessary to prevent its leakage to the working area. The catalytic oxidation and adsorption is the most reliable method to recover tritium released into the working area of those facilities. Therefore, there is a necessity that the tritium recovery system with large-scale and higher integrity is developed and constructed. For this purpose, it is required to obtain and accumulate updated database for chemical engineering design based on most recently commercial and available catalysts and absorbents. In this work, we selected a catalyst and an adsorbent, and examined their adsorption characteristics for water vapor and performance of catalytic oxidation of hydrogen. Adsorption isotherms were studied with a volumetric gas adsorption instrument. Various adsorption models were tested to correlate the experimental isotherms. Breakthrough experiments were also performed to assess adsorption performances. Furthermore, numerical simulations were performed based on the obtained experimental results.

Keywords: detritiation, catalyst, adsorbent, membrane dehumidifier, numerical simulation, mass balance

1. Introduction

A large amount of tritium would be handled as fuel in nuclear fusion power plants. In these facilities, tritium is confined in multiple confinement barriers. However, if unexpected accidents take place, tritium leaks to the working areas. Thus, establishment of tritium recovery system is necessary to prevent its leakage to the working area. The catalytic oxidation and adsorption is the most reliable method to recover tritium released into the working area of those facilities. In this method, tritium gas is oxidized with catalysts, and then tritiated water vapor is collected by adsorbents.

It is planned to conduct deuterium plasma experiments in National Institute for Fusion Science (NIFS). In these experiments, D-D fusion reactions take place and tritium is produced, and thus the release of tritium to the environment has to be minimized. Therefore, there is a necessity that the tritium recovery system with large-scale and higher integrity is developed and constructed. However the previous experimental and engineering database [1] obtained by several researchers on absorbents cannot be applied to the design of updated tritium recovery system since the absorbents used in the previous studies are not been produced any longer in the industry. Therefore, it is required to obtain and accumulate updated database for chemical engineering design by testing most recently commercial and available catalysts and absorbents in experiments. In this work, we selected an adsorbent and examined its adsorption characteristics for water vapor.

2. Catalyst and adsorbent

The authors went through previous literature and inquired about catalysts or adsorbents used for detritiation systems that are being used in several research institutes. However, the result of such survey reveals that the production or model number of the materials such as catalyst and adsorbent is not clear, and they are not considered to be available in the present industrial market. Additionally, conduction of new screening tests, in order to search feasible catalysts or adsorbents, is time consuming. It should be also noted that feasibility tests of catalysts and adsorbents are not limited within catalytic activity or adsorption performance; durability in long-time use, mechanical stability, ease in their procurement with large quantities are important points as well.

For this reason, the authors selected a catalysts and an adsorbent, which are ones of the most widely and generally used in industries and are credited and reputed by engineers and designers as well.

In terms of catalyst, the authors selected a Pt/alumina catalyst, DASH520, manufactured by N. E. Chemcat Co., which is widely used in industries for various purposes. The catalyst was deposited with 4.1g/L of platinum. The average diameter of the catalyst is 3.25 mm. the packing density was 770 g/L.

With regard to the adsorbent, the author selected a MS5A adsorbent that is produced by Union Showa Co. in Japan (subsidiary company of Union Carbide Co.) and is widely used in industries. The production of zeolites in Union Showa Co. is licensed by Union Carbide Co, and the pellet-type MS5A adsorbent could be one of the world-standard adsorbents.

Corresponding author: kenzo@gipc.akita-u.ac.jp

©2013 by The Japan Society of Plasma Science and Nuclear Fusion Research

3. Experimental

3.1 Catalytic oxidation of hydrogen

The experiments were performed under the steady state condition. The catalysts were packed in a reactor made of quartz. The temperature of the reactor was controlled with the constant temperature bath. Argon gas was used as a carrier gas. The argon gas containing hydrogen (about 300-800 ppm) and oxygen (20%) was introduced to the reactor.

Experiments were also performed using wet process gases which contained water vapor (about 300-1000 Pa) in order to study the influence of coexistent water vapor on the catalytic activity for oxidation of hydrogen. The concentrations of hydrogen at inlet and outlet stream of the reactor were measured with a gas-chromatograph (GC-8A) manufactured by SHIMAZU Co.

3.2 Water adsorption

The authors studied adsorption behavior of water vapor on the DASH520 catalyst and MS5A adsorbent, as well. The adsorption isotherms of water vapor on the DASH520 catalyst and MS5A adsorbent were measured using a volumetric gas adsorption instrument, BELSORP-max, manufactured by BEL Japan Inc. The instrument is designed for measurement of wide range of adsorption isotherms on surface area and pore size distribution analysis.

3.3 Summary of experimental results

Conversion rate R_c and over all mass transfer capacitance for oxidation (based on surface reaction) in dry condition $k_{r,ox,0}$a were computed to assess catalytic performance. R_C and $K_{F,ox}$ are defined as

$$S_V = Q / V \tag{1}$$

$$R_C = 100 \times (C_{in} - C_{out}) / C_{in} \tag{2}$$

Table 1 Parameters optimized for L-F equation.

	m	DASH520	MS5A
$q_{s,m}$ [mol/g]	1	1.52×10^{-4}	19.8
$b_{0,m}$ [(mol/(g·Pa))$^{1/u_i}$]		3.86×10^{-13}	2.02×10^{-15}
E_m [J/(mol·K)]		39100	44700
v_m [-]		3.16	0.908
$q_{s,m}$ [mol/g]	2	4.58	0.00703
$b_{0,m}$ [(mol/(g·Pa))$^{1/u_i}$]		1.49×10^{-22}	8.90×10^{-20}
E_m [J/(mol·K)]		75100	92000
v_m [-]		1.76	2.67
$q_{s,m}$ [mol/g]	3	3.57×10^{-4}	0.00191
$b_{0,m}$ [(mol/(g·Pa))$^{1/u_i}$]		1.43×10^{-7}	1.42×10^{-9}
E_m [J/(mol·K)]		38800	36100
v_m [-]		3.25	4.05
$q_{s,m}$ [mol/g]	4	1.70×10^{-5}	0.000485
$b_{0,m}$ [(mol/(g·Pa))$^{1/u_i}$]		6.62×10^{-10}	4.98×10^{-12}
E_m [J/(mol·K)]		34800	64400
v_m [-]		1.93	6.33
$q_{s,m}$ [mol/g]	5	2.12×10^{-3}	-
$b_{0,m}$ [(mol/(g·Pa))$^{1/u_i}$]		9.85×10^{-9}	-
E_m [J/(mol·K)]		32800	-
v_m [-]		2.09	-

$$k_{r,ox,0}a = S_V \ln\left(C_{in} / C_{out}\right) \tag{3}$$

The mass transfer capacitances for oxidation of hydrogen (based on surface reaction) of DASH520 is expressed as

$$k_{r,ox,0}a = 1.16\times10^5 \exp\left(-25400/(RT)\right) \tag{4}$$

The experimental adsorption isotherms of water vapor on the DASH520 catalyst and MS5A adsorbent were found to be successfully correlated using a sort of multi-site Langmuir-Freundrich equation:

$$q_{ad} = \sum_{m=1}^{n} \frac{q_{ad,s,m} b_m p^{v_m}}{1 + b_m p^{v_m}} \tag{5}$$

$$b_m = b_{0,m} \exp(E_m / RT) \tag{6}$$

Parameters (optimized by non-linear least squares analysis) for DASH520 catalyst (n=5) and MS5A adsorbent (n = 4) are listed in Table 1.

Experimental results on the catalytic oxidation of hydrogen in wet gases reveal that coexistence of water vapor severely inhibits the catalytic oxidation of hydrogen. It was found that the mass transfer coefficient for catalytic oxidation in wet gases is expressed as a function of the amount of water adsorbed on the catalyst substrate:

$$\frac{k_{r,ox}a}{k_{r,ox,0}a} = 0.476\exp\left[-\left(643 q_{ad}\right)^{25.1}\right] + 0.524\exp\left[-\left(456 q_{ad}\right)^{5.00}\right] \tag{7}$$

4. Simulation procedure and mass balance

The basic assumption on catalyst and adsorption bed is one-dimensional dispersed plug flow in packed bed [2]. Chemical reactions such as catalytic oxidation of hydrogen isotopes, adsorption of water vapor, isotope exchange reaction were taken into consideration. The mass balance equations in catalyst beds are expressed as follows (for adsorption bed, catalytic reactions are not considered):

・Mass balance of Q_2 (i = H, D or T) in gas phase

$$\frac{\partial(uC_{Q2,i})}{\partial z} + \varepsilon\frac{\partial C_{Q2,i}}{\partial t} + \varepsilon\frac{\partial}{\partial z}\left(D_L \frac{\partial C_{Q2,i}}{\partial z}\right) = -k_{F,ox} a C_{Q2,i} \tag{8}$$

$$\frac{1}{k_{F,ox}a} = \frac{1}{k_{r,ox}a} + \frac{1}{k_g a} \tag{9}$$

・Mass balance of Q_2O (i = H, D or T) in gas phase

$$\frac{\partial(uC_{Q2O,i})}{\partial z} + \varepsilon\frac{\partial C_{Q2O,i}}{\partial t} + \varepsilon\frac{\partial}{\partial z}\left(D_L \frac{\partial C_{Q2O,i}}{\partial z}\right) \tag{10}$$

$$= k_{F,ox} a C_{Q2,i} - k_{F,ad,i} a \left(c_{Q2O,H} + c_{Q2O,D} + c_{Q2O,T} \right) \theta_1 + k_{F,ex} a \theta_2$$

・Mass balance of Q_2O (i = H, D or T) in solid phase

$$\gamma \frac{\partial \bar{q}_{Q2O,i}}{\partial z} = k_{F,ad,i} a \left(c_{Q2O,H} + c_{Q2O,D} + c_{Q2O,T} \right) \theta_1 - k_{F,ex} a \theta_2 \tag{11}$$

$$\bar{q}_{Q2O,i} = q_{ad,Q2O,i} + q_{st,Q2O,i} \tag{12}$$

$$\theta_1 = c_{Q2O,i} - \frac{\left(c_{Q2O,H} + c_{Q2O,D} + c_{Q2O,T} \right) \bar{q}_{Q2O,i}}{\bar{q}_{Q2O,H} + \bar{q}_{Q2O,D} + \bar{q}_{Q2O,T}} \tag{13}$$

$$\begin{aligned} &when\ \ c_{Q2O,H} + c_{Q2O,D} + c_{Q2O,T} \geq 0 \\ &\theta_2 = c_{Q2O,i} / \left(c_{Q2O,H} + c_{Q2O,D} + c_{Q2O,T} \right) \\ &when\ \ c_{Q2O,H} + c_{Q2O,D} + c_{Q2O,T} < 0 \\ &\theta_2 = \bar{q}_{Q2O,i} / \left(\bar{q}_{Q2O,H} + \bar{q}_{Q2O,D} + \bar{q}_{Q2O,T} \right) \end{aligned} \tag{14}$$

The heat balance equation is given as

$$\begin{aligned} &\frac{\partial \left(u \rho_g c_{p,g} T \right)}{\partial z} + \varepsilon \frac{\partial \left(\rho_g c_{p,g} T \right)}{\partial t} + \gamma \frac{\partial \left(c_{p,s} T \right)}{\partial t} \\ &+ \frac{\partial}{\partial z} \left(\lambda_{eff} \frac{\partial T}{\partial z} \right) \\ &= (k_{F,ox,H} C_{Q2,H} + k_{F,ox,D} C_{Q2,D} + k_{F,ox,T} C_{Q2,T}) a \Delta H_{ox} \\ &+ k_{F,ad,T} a (C_{Q2O,H} + C_{Q2O,D} + C_{Q2O,T} - C^*) \Delta H_{ad} \\ &- 4 h_w (T - T_{air}) / D_b \end{aligned} \tag{15}$$

The assumptions used in the modeling of membrane dehumidifier are: (i) the feed gas is a binary mixture of water vapor and air, (ii) the pressure drops and diffusive mass transfer in the feed side and permeation side are negligible, (iii) laminar films on the surface of the membrane are negligible and (iv) the system is adiabatic and the temperature of the gas mixture is constant [3]. The molar fluxes of penetrants through the dense and porous layers can be expressed as,

$$N_{d,i} = D_{d,i} \frac{dC_{d,i}}{dl} = \frac{D_{d,i} S_w}{\delta_d} \left(p_{h,i} - p_{l,i} \right) = P_{d,i} \left(p_{h,i} - p_{l,i} \right), \tag{16}$$

$$N_{2,i} = D_{2,i} \frac{dC_{2,i}}{dl}. \tag{17}$$

In Eq. (16), a constant pressure gradient is assumed and a permeance is applied because the thickness of the dense layer is very thin and the value is not disclosed by the vendor. The diffusion coefficient $D_{2,i}$ in Eq. (17) is estimated as Knudsen's diffusion coefficient.

Polyimide membranes absorb moisture easily at high pressures of water vapor. The sorption capacity of water vapor in equilibrium increases almost linear with the activity of water vapor [5]. In the present study, water vapor content in the matrix of support layer in equilibrium is expressed by the following equation.

$$\bar{C}'_{2,w} = a_{sorp} \left(p_{2,w} / p_s \right) \tag{18}$$

Sorption rate of water vapor is, then, expressed as

$$r = \varepsilon V'_2 k_{sorp} \left(\bar{C}'_{2,w} - C'_{2,w} \right). \tag{19}$$

It is known that a very low partial pressure of a condensable species, such as water vapor in the feed stream, can significantly reduce the permeability of the other constituent relative to its permeability as a pure component. In the present study, the permeance of air is expressed by the following equation at relatively low water vapor activity.

$$P_{d,a} = P_{d,a,0} - a_p \left(p_{h,w} / p_s \right) \tag{20}$$

The membrane is divided into small sections along the axis, and a kind of plate model was applied. The total mass balances are expressed as

$$V_{1,j} \frac{dC_1}{dt} = 0 = q_{1,j} - q_{1,j+1} - N_{12,j} S_1, \tag{21}$$

$$\varepsilon V_{2,j} \frac{dC_{2,j}}{dt} = N_{12,j} S_1 - N_{23,j} S_2 - r_j \tag{22}$$

and

$$V_{3,j} \frac{dC_3}{dt} = 0 = q_{3,j+1} - q_{3,j} + N_{23,j} S_2. \tag{23}$$

The mass balances for each component are, then,

$$V_{1,j} C_1 \frac{dx_{1,j}}{dt} = q_{1,j} x_{1,j} - q_{1,j+1} x_{1,j+1} - N_{12,w,j} S_1, \tag{24}$$

$$\varepsilon V_{2,j} \frac{dC_{2,w,j}}{dt} = N_{12,w,j} S_1 - N_{23,w,j} S_2 - r_j, \tag{25}$$

$$\varepsilon V_{2,j} \frac{dC_{2,a,j}}{dt} = N_{12,a,j} S_1 - N_{23,a,j} S_2, \tag{26}$$

$$(1 - \varepsilon) V_{2,j} \frac{dC'_{2,w,j}}{dt} = r_j \tag{27}$$

and

$$V_{3,j} C_3 \frac{dx_{3,j}}{dt} = q_{3,j+1} x_{3,j+1} - q_{3,j} x_{3,j} + N_{23,w,j} S_2. \tag{28}$$

Equations (25) and (26) represent the mass transfers in the pore of the support layer. On the other hand, Eq. (27) represents the concentration change of water vapor in the matrix of the support layer. Equations (29)-(31) and the relationships, $N_{12,w,j} = N_{A,w} = N_{B,w}$ and $N_{23,w,j} = N_{C,w}$ give Eqs. (32) and (34) as fluxes in which the mass conservations across the membrane is taken into account. In the same way, Eqs. (33) and (35) are obtained for the air.

$$N_{A,w} = \frac{D_{d,w}}{\delta_d} \left(S_w p_h x_{1,j} - S_w C^{int}_{2,w,j} RT \right) = P_{d,w} \left(p_h x_{1,j} - C^{int}_{2,w,j} RT \right) \tag{29}$$

$$N_{B,w} = \frac{2D_{2,w}}{\delta_2}\left(C_{2,w,j}^{int} - C_{2,w,j}\right) \quad (30)$$

$$N_{C,w} = \frac{2D_{2,w}}{\delta_2}\left(C_{2,w,j} - \frac{p_l x_{3,j}}{RT}\right) \quad (31)$$

$$N_{12,w,j} = \frac{2D_{2,w}P_{d,w}}{P_{d,w}\delta_2 RT + 2D_{2,w}}\left(p_h x_{1,j} - C_{2,w,j}RT\right) \quad (32)$$

$$N_{12,a,j} = \frac{2D_{2,a}P_{d,a}}{P_{d,a}\delta_2 RT + 2D_{2,a}} \times \left\{p_h\left(1 - x_{1,j}\right) - C_{2,a,j}RT\right\} \quad (33)$$

$$N_{23,w,j} = \frac{2D_{2,w}}{\delta_2 RT}\left(C_{2,w,j}RT - p_l x_{3,j}\right) \quad (34)$$

$$N_{23,a,j} = \frac{2D_{2,a}}{\delta_2 RT}\left\{C_{2,a,j}RT - p_l\left(1 - x_{3,j}\right)\right\} \quad (35)$$

$$N_{12,j} = N_{12,w,j} + N_{12,a,j} \quad (36)$$

$$N_{23,j} = N_{23,w,j} + N_{23,a,j} \quad (37)$$

The mass balance equations discredited and then matrices generated were solved by direct methods such as LU decomposition method. The generalized Crank-Nicholson scheme was applied for time-marching procedure.

5. Results and discussion

5.1 Detritiation system design of NIFS

In D-D experiments in NIFS, (a) detritiation of downstream of outgas generated in cleaning of plasma container (vacuum vessel purge gas) and (b) plasma exhaust gases is required. Thus, it is necessary to develop a detritiation system to recover low-concentration tritium generated in LHD (Large Helical Device). The schematics of the detritiation system designed at present are shown in Fig. 1. Representative operational conditions are summarized in Table 2. With regard to the vacuum vessel purge gas, the process gas is first introduced to 100 kg of catalyst bed and then tritiated water vapor is collected by condenser and polymer membrane-type dehumidifier. In contrast, the plasma exhaust gases are treated using catalyst and adsorption beds. One of the major differences is throughput of the gases processed. The concentrations of tritium and deuterium are considerably higher in the plasma exhaust gas. Numerical simulations were performed for both cases described above.

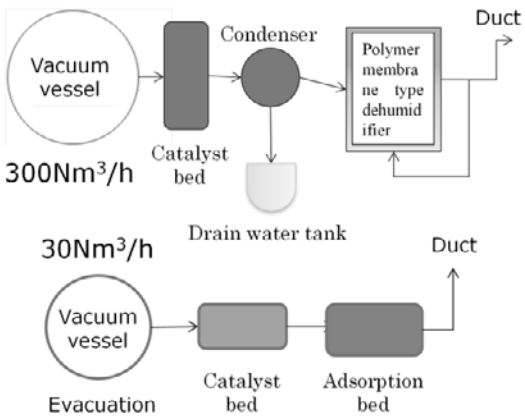

Fig. 1 Detritiation systems designed in NIFS

(a) outgas generated in cleaning of plasma container
(b) downstream of plasma exhaust gases.

Table 2 Operational condition of detritiation system.

Detritiation of vacuum vessel purge gas	Detritiation of plasma exhaust
$C_{Q2,H}$: 0.5 ppm	$C_{Q2,H}$: 130.0ppm
$C_{Q2,D}$: 90.0 ppm	$C_{Q2,D}$: 2983.3 ppm
$C_{Q2,T}$: 1×10^{-8} ppm	$C_{Q2,T}$: 9.25×10^{-6} ppm
$C_{Q2O,H}$: 1500.0 ppm	$C_{Q2O,H}$: 3.6667 ppm
$C_{Q2O,D}$: 90.0 ppm	$C_{Q2O,D}$: 28.667 ppm
$C_{Q2O,T}$: 1×10^{-8} ppm	$C_{Q2O,T}$: 6×10^{-8} ppm
Amount of catalyst: 100 kg	Amount of catalyst: 100 kg
Temp. of catalyst: 30℃, 100℃, 200℃	Temp. of catalyst: 30℃, 100℃, 200℃, 400℃
Heating: heat exchanger, adiabatic	Heating: heat exchanger, adiabatic
Recovery: Polymer membrane-type dehumidifier UM-XC5 (Φ90 mm×710 mm), 60 sets, high pressure 0.6 MPa, low presasure0.1 MPa, 30 ℃, 100 L/min	Recovery: MS5A adsorbent,100 kg
Dehumidifier cooling: heat exchanger, adiabatic	Adsorbent cooling: heat exchanger, adiabatic

5.2 Results of numerical simulation for detritiation of vacuum vessel purge gas

Figure 2 shows changes in the concentration of molecular form of tritium in the outlet stream of the catalyst bed. With regard to the temperature of inlet gas, three cases (30 °C, 100 °C and 200 °C) were tested. It can be seen in the figure that catalytic activity is considerably decreased in the cases where the inlet gas temperatures are 30 °C and 100 °C. This is because that water vapor contained in the process gas inhibits

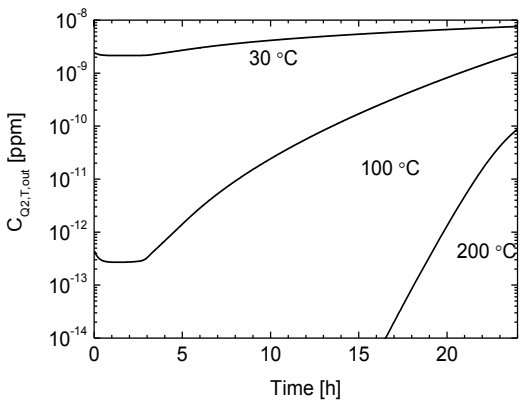

Fig. 2 Change in concentration T_2 in outlet stream of Pt/alumina catalyst beds.

catalytic activity with increase in the amount of water adsorbed on the catalyst substrate. However, this effect could be considerably avoided if the inlet gas temperature is raised to 200 °C as shown in the figure. Thus, preheating of the process gas with heat exchangers is necessary for the treatment of vacuum vessel purge gas.

Subsequent numerical simulation for condenser and polymer membrane-type dehumidifier was performed in the case where the inlet gas temperature is raised to 200 °C. The transient variations of chemical components such as hydrogen isotopes and isotopes of water vapor in the outlet stream of the catalyst bed were used as the inlet condition of the polymer membrane-type dehumidifier. Figure 3 shows changes in amounts of bulk water and concentration of tritiated water in drain tank. The amount of bulk water increases almost linearly with lapse time. The concentration of tritiated water increases in the same trend. Figure 4 shows changes in concentrations of molecular form of tritium and tritiated water vapor at the outlet of the duct. The concentration of tritiated water vapor increases almost linearly with lapse time. The molecular form of tritium sharply increases 20 h after the commencement of operation of the detritiation system, since the inhibition of catalytic activity by water vapor becomes a dominant factor. However, the result of this simulation indicates that regulatory level of tritium concentration at the outlet of the duct is fulfilled.

5.3 Results of numerical simulation for detritiation of plasma exhaust gas

Figure 5 (a) shows changes in T_2 concentration in outlet stream of the catalysts bed. In this case, preheating of the process gas before the catalyst bed is unnecessary because of the help of higher concentration of D_2; its reaction can generate heat and raise the reactor

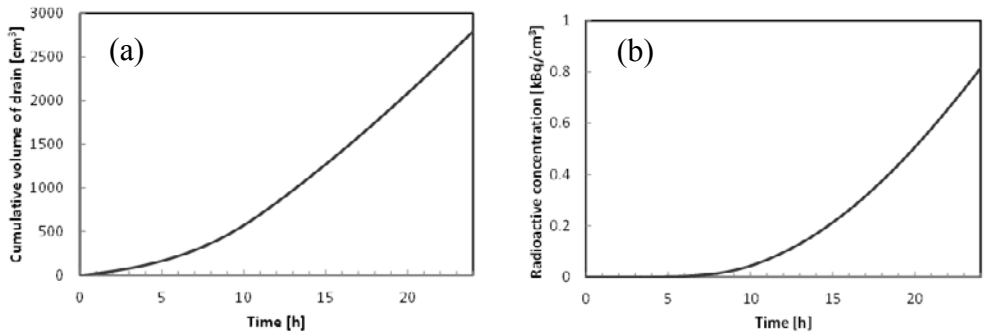

Fig. 3 Change in (a) amount of bulk water and (b) concentration of tritium in drain tank.

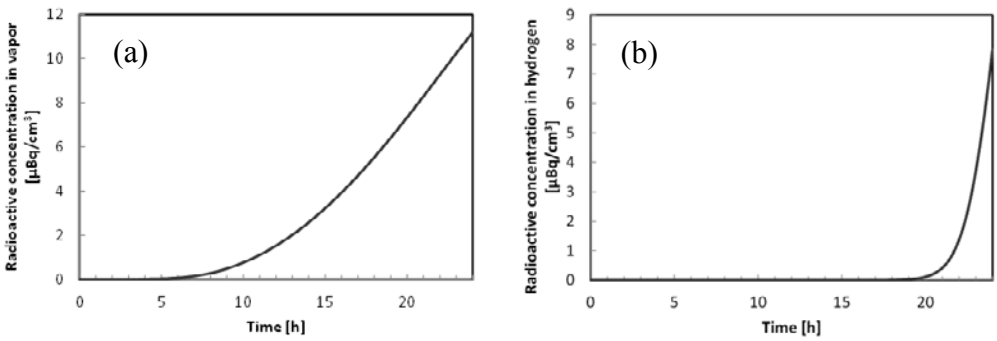

Fig. 4 Change in (a) concentration of molecular form of tritium
and (b) concentration of tiritiated water vapor on outlet stream of duct.

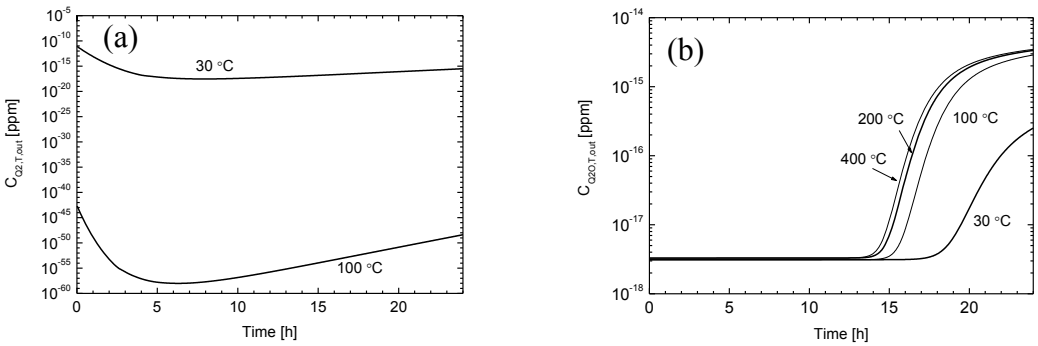

Fig. 5 Change in (a) concentration of molecular form of tritium in outlet gas of catalysts bed
and (b) concentration of tiritiated water vapor on outlet stream of adsorption bed.
(Temperatures shown in the figures represent the temperature of the process as at inlet of the catalyst bed.)

temperature. Figure 5 (b) shows breakthrough curve for T_2O vapor, which indicates that breakthrough starts at 10 h after the start of operation of 100 kg of MS5A adsorbent regardless of variation in temperature of process gas at the inlet of the catalyst bed.

6. Conclusion

Catalytic oxidation rate of hydrogen and water adsorption characteristics are investigated with regards to commercial catalyst and adsorbent. Based on the experimental results, simulation models were constructed for catalyst bed, adsorption bed and polymer-type membrane dehumidifier. Test process simulations were carried out on the basis of the detritiation systems designed in NIFS.

Nomenclature

a	Specific surface area [m^2 m^{-3}]
a_{sorp}	Slope of the adsorption isotherm [mol m^{-3}]
a_p	Coefficient in Eq. (20) [mol m^{-2} s^{-1} Pa^{-1}]
b_0	Constant related to Langmuir-Freundrich equation [arbitrary]
$c_{p,g}$	Specific heat of gas [J g^{-1} K-1]
$c_{p,s}$	Specific heat of solid phase [J kg^{-1} K-1]
C	Molar concentration [mol m^{-3}]
D	Diffusion coefficient [m^2 s^{-1}]
D_b	Bed diameter [m]
ΔH_{ad}	Adsorption heat [J mol^{-1}]
ΔH_{ox}	Reaction heat for catalytic oxidation [J mol^{-1}]
$k_{F,ad}$	Overall mass transfer coefficient for adsorption [m/s]
$k_{F,ox}$	Overall mass transfer coefficient for catalytic oxidation [m/s]
K_g	Mass transfer coefficient for gas film layer [m/s]
$k_{r,ox}$	Mass transfer coefficient for catalytic oxidation based on surface reaction [m/s]
$k_{r,ox,0}$	Mass transfer coefficient for catalytic oxidation based on surface reaction in dry condition[m/s]
k_{sorp}	Rate constant of the adsorption [s^{-1}]
l	Position in the permeate direction [m]
N	Permeation flux [mol m^{-2} s^{-1}]
p	Pressure or partial pressure [Pa]
P	Permeance [mol m^{-2} s^{-1} Pa^{-1}]
q	Flow rate [mol s^{-1}]
q_{ad}	Concentration of water adsorbed [mol g^{-1}]
q_{st}	Concentration of water strongly bound to surface (structural water) [mol g^{-1}]
$\bar{q}$	Net Concentration of water species on the surface [mol g^{-1}]
Q	Volumetric gas velocity [m^3 s^{-1}]
r	Adsorption rate of water vapor [mol s^{-1}]
R	Gas constant [J K^{-1} mol^{-1}]
R_c	Conversion rate [-]
S	Outside wall area of a calculation cell [m^2]
S_V	Space velocity [s^{-1}]
S_w	Solubility coefficient of water [mol m^{-3} Pa^{-1}]
t	Time [s]
T	Temperature [K]
u	Superficial gas velocity [m s^{-1}]
V	Volume [m^3]
V	Constant related to Langmuir-Freundrich equation [-]
X	Mole fraction of water vapor [-]
Z	Length in axial direction [m]

Greek letters

Δ	Thickness of the layer [m]
E	Void ratio in the porous layer
λ_{eff}	Effective heat conductivity in axial direction [J m^{-1} s^{-1}]
ρ_g	Density of gas [g m^{-3}]

Overscript

Int	Interface between dense and porous layer
$\bar{}$	Equilibrium state
$'$	Matrix of the porous layer

Subscripts

0	Initial value
1	Feed side
12	From feed side to the porous layer
2	Porous layer
23	From porous layer to the permeation side
3	Permeation side
A	Air
A	Indicator in Fig. 2
B	Indicator in Fig. 2
C	Indicator in Fig. 2
D	Dense layer
H	High pressure side
I	Component (H, D or T) or (w or a)
In	inlet
J	Number of the calculation cell along the axis
L	Low pressure side
M	Adsorption site number
N	Maximum adsorption site number
Out	outlet
Q	H, D, or T (^1H, ^2H or ^3H)
S	Saturated state
W	Water vapor

References

[1] K. Kotoh and K. Kudo, "Applicability of Commercial Adsorbents to Multi-column Adsorption Systems with Condenser for Tritiated Water Vapor Removal", Journal of Nuclear Science and Technology, 34, 1099(1997)

[2] K. Munakata, M. Nishikawa, T. Takeishi, N. Mitsuishi and M. Enoeda, "Recovery of Tritium in Room Air by Precious Metal Catalysts with Hydrophilic Substrate", Journal of Nuclear Science and Technology. 25 , 383 (1988)

[3] T. Sugiyama, N. Miyahara, M. Tanaka, K. Munakata and I. Yamamoto, "A Simulation Model for Transient Response of A Gas Separation Module Using A Hollow Fiber Membrane", Fusion Engineering and Design, 86, 2743(2011).